Available online at www.sciencedirect.com
ScienceDirect
Mendeleev Commun., 2014, **24**, 298–300
Mendeleev Communications

3-Carboxy-2,2,5,5-tetra($^2H_3$)methyl-[4-^{2}H(^{1}H)]-3-pyrroline-(1-^{15}N)-1-oxyl as a spin probe for *in vivo* L-band electron paramagnetic resonance imaging

Leonid A. Shundrin,*[a,b,c] Igor A. Kirilyuk[a,b] and Igor A. Grigor'ev[a,d]

[a] *N. N. Vorozhtsov Novosibirsk Institute of Organic Chemistry, Siberian Branch of the Russian Academy of Sciences, 630090 Novosibirsk, Russian Federation. Fax: +7 383 330 9752; e-mail: shundrin@nioch.nsc.ru*
[b] *Department of Natural Sciences, Novosibirsk State University, 630090 Novosibirsk, Russian Federation*
[c] *Scientific Institute of Clinical and Experimental Lymphology, 630060 Novosibirsk, Russian Federation*
[d] *E. N. Meshalkin State Research Institute of Circulation Pathology, 630055 Novosibirsk, Russian Federation*

DOI: 10.1016/j.mencom.2014.09.017

The suitability of 3-carboxy-2,2,5,5-tetra($^2H_3$)methyl-[4-^{2}H(^{1}H)]-3-pyrroline-(1-^{15}N)-1-oxyl and its non-deuterated ^{14}N-containing nitroxide analogue for L-band EPR *in vivo* imaging has been demonstrated. Both nitroxides exhibit low rates of reduction with ascorbate and slow decay in mice blood and plasma and, according to the EPR data, accumulate in the liver of a living mice within 10–70 min after the injection *via* tail vein, and then collect in the bladder.

Electron paramagnetic resonance imaging (EPRI) is an emergent kind of magnetic resonance tomography.[1] Nitroxides possess many desirable qualities as EPR probes, including ease of preparation, variability of chemical structure and high sensitivity to physiological parameters, including O_2 concentration in various tissues, extracellular pH and tissue redox status.[2,3] The EPR spectra of ^{15}N-labeled nitroxide radicals (NRs) with deuterated methyl groups adjacent to the nitroxide fragment are characterized by two lines in ^{15}N hyperfine structure with more narrow lines as compared with the spectra of widely used non-deuterated ^{14}N-nitroxide spin probes.[1,2] These features make the use of ^{15}N- and ^{2}H-substituted NR as specific spin probes for *in vivo* EPR based oximetry[3] and EPRI techniques[4] advantageous compared to conventional non-deuterated nitroxide spin probes. NRs have limited stability *in vivo* due to reduction with low-molecular antioxidants (ascorbate, thiols, *etc*.) and enzymatic systems, and intracellular reduction plays the major role.[5] 3-Carboxy-2,2,5,5-tetramethyl-3-pyrroline-1-oxyl **2** (Figure 1) is moderately resistant to reduction with ascorbate, showing the rate constant k_{asc} = 0.22 dm^3 mol^{-1} s^{-1} (in a hydrocarbonate buffer with pH 7.2).[6] However, **2** is a relatively strong acid (pK 3.5)[7] existing in the anionic form within a physiological range of pH. The anion of **2** obviously has low permeability *via* cellular membranes, remaining predominantly in extracellular space, and this should make the nitroxide resistant to reduction *in vivo*. We studied the properties of **2** and its deuterated and ^{15}N-containing analogue, 3-carboxy-2,2,5,5-tetra-($^2H_3$)methyl-[4-^{2}H(^{1}H)]-3-pyrroline-(1-^{15}N)-1-oxyl **1** (Figure 1) as a spin probe for L-band EPRI of laboratory mice.

Nitroxide **1** was prepared from fully deuterated (^{15}N) triacetonamine without special precautions to prevent deuterium to protium exchange during bromination and Favorskii rearrangement (Scheme 1).†

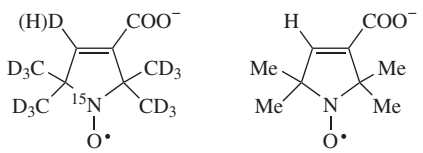

4-position: **1a** D (~73%) **1b** H (~27%) **2**

Figure 1 Structures of spin probes **1a**,**b**, **2** (anionic forms).

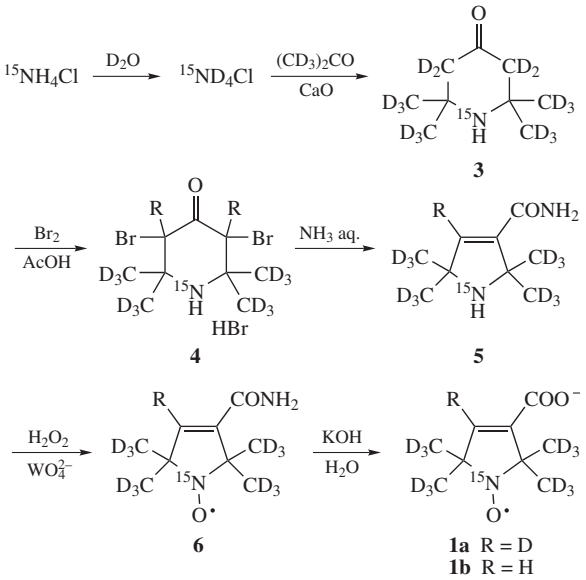

Scheme 1

† *4-Oxo-2,2,6,6-tetra($^2H_3$)methyl-(3,3,5,5-$^2H_4$,1-^{15}N)piperidine* **3** was prepared following the general procedure of Pirrwitz and Schwarz[12] with minor modifications. To generate $^{15}ND_4Cl$, $^{15}NH_4Cl$ (Isotec, enrichment 98+%, 10 g) was dissolved in D_2O (99.9, 15 ml); the solution was evaporated to dryness in a vacuum. This procedure was repeated five times.[4] The $^{15}ND_4Cl$ (4 g, 71 mmol), freshly annealed CaO (4 g, 71 mmol), acetone-d_6 (20 ml, 272 mmol) and 5 to 10 metal balls (*ca*. 0.5 g each), covered with thick layer of polyethylene, were placed in the thick-wall 40–50 ml bottle equipped with a waterproof stopper. The bottle was sealed and vigorously shaken until the precipitate stick together into a viscous mass. The bottle was placed in a water bath, and the temperature was gradually increased to 60 °C in 24 h. The bottle was shaken vigorously at regular intervals at 60 °C during 170–200 h. Then, the mixture was allowed to cool down to room temperature, the bottle was opened, the mixture was diluted with hexane (30 ml) and the solution was separated *via* decantation. The inorganic precipitate was then extracted with diethyl ether (10×30 ml). The solvents were carefully distilled off from the combined extracts (the product is volatile!), the residue was dissolved in CCl_4 and placed in a refrigerator (–18 °C). The crystalline precipitate was filtered off and washed with a small amount of cold CCl_4 to yield 5.5 g (50%) of **3**. Additional portion of **3** can be isolated from mother liquor using column chromatography on Al_2O_3.

The X-band EPR spectra of compounds **1** and **2** (for the spectral parameters, see Table S1, Online Supplementary Materials) in a 50 mM phosphate buffer (pH 7.4) are shown in Figure 2. The EPR spectrum of **1** is a superposition of the spectra of **1a** and **1b**. No hyperfine interaction (HFI) with the residual proton in the 4-position was observed for nitroxide **1**, even for its solution (0.2 mM) in an oxygen-free buffer (Figure S1),‡ on the contrary to the spectra of 3-carbamoyl-2,2,5,5-tetra($^2H_3$)methyl-3-(1-^{15}N) pyrroline-1-oxyl.[8] Noticeable differences in line widths in the EPR spectra of **1** [Figure 2(*a*), Table S1‡] are observed because of the modulation of anisotropic HFI with ^{15}N nucleus caused by the rapid rotational diffusion of **1** in solution. Nitroxide **2** has a typical three line EPR spectrum [Figure 2(*b*)], which is characterized by broader lines in comparison with **1** (Table S1).

The *in vitro* reduction of **1** and **2** by the ascorbate anion in a phosphate buffer with pH 7.4 [Figure 2(*c*), example for **1**] proceeds with slow and similar rates.§ Corresponding bimolecular rate constants are almost independent on isotope enrichment and were found to be 0.152±0.007 and 0.145±0.05 dm^3 mol^{-1} s^{-1}, which are lower than the corresponding rate constants for six-membered ring nitroxides (3.5 dm^3 mol^{-1} s^{-1} for TEMPO,[9] 7.0 dm^3 mol^{-1} s^{-1} for TEMPOL[10]) and comparable with those for five-membered ring nitroxides (0.07–0.3 dm^3 mol^{-1} s^{-1}).[9,11]

The kinetics of reduction of **1** in mouse blood and plasma [Figure 2(*d*)] shows the linear time dependence of the concentration of **1**, which is in agreement with the total zero order of reduction kinetics. The cell permeability of **1** is expected to be low. As a consequence, a decrease in the concentration of **1** by 9 and 5% is observed during 66 min under the reduction in blood and plasma, respectively. The reduction of **2** under the same conditions exhibits close characteristics. Thus, nitroxides **1** and **2** possess high resistance to reduction by blood and plasma *in vitro* and this makes reasonable testing them as spin probes for *in vivo* EPRI.

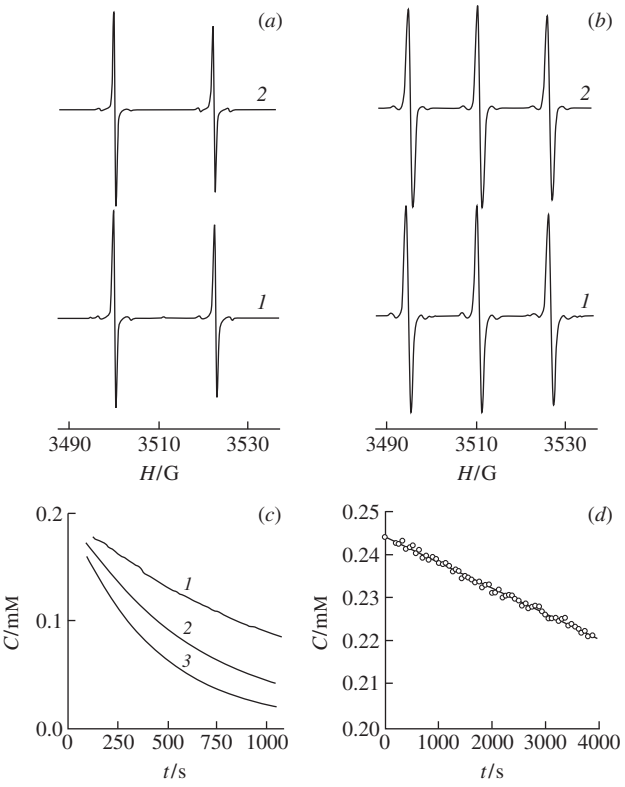

Figure 2 X-band EPR spectra of (*a*) **1** and (*b*) **2** in a phosphate buffer (pH 7.40): (*1*) experiment, (*2*) simulation, and *in vitro* reduction kinetics of **1** with the ascorbate anion (AscH$^-$) (*c*): (*1*) 5, (*2*) 10 and (*3*) 15 mM and (*d*) in mouse blood.

To testify **1** and **2** as spin probes for L-band EPR tomography¶ of laboratory animals, 300 μl of 75 mM solutions of the spin probes in a standard physiological buffer were infused in previously anesthetized laboratory male mice *via* tail vein.†† EPR images with **1** as a spin probe were obtained 10 min after injection in up-to-down (*zx*) [Figure 3(*c*)] and front-to-back (*zy*) [Figure 3(*b*)] projections one after another. EPR images obtained with FOV1 [Figure 3(*a*)] demonstrate the accumulation of **1** in mouse liver, the two parts of a liver are distinctly observed at both EPRI projections. The *zy* image obtained with nitroxide **2** as a spin probe using the same parameters of EPRI registration displays lower resolution [Figure 3(*d*)]. The resolved EPR images with FOV1 can be obtained during the time interval 10–70 min after the injection of **1** and **2**. Within this time, the concentrations

3-Carboxy-2,2,5,5-tetra($^2H_3$)methyl-[4-^{2}H(^{1}H)]-3-pyrroline-(1-^{15}N)-1-oxyl **1**. All subsequent steps of the synthesis of **1** were performed in non-deuterated solvents in accordance with procedures for ^{14}N, non-deuterated compounds.[13] A MicrOTOF-Q hybrid quadrupole time-of-flight mass spectrometer (Bruker Daltonics) was used for MS analysis. MS, *m*/*z* (%): 195.160 (5.3), 196.167 (43.4), 197.173 (100), 198.176 (9.8). Assuming that the resulting nitroxide is a mixture of fully deuterated 3-carboxy-2,2,5,5-tetra($^2H_3$)methyl-(4-^{2}H)-3-pyrroline-(1-^{15}N)-1-oxyl **1a** and partly deuterated 3-carboxy-2,2,5,5-tetra($^2H_3$)methyl-(4-^{1}H)-3-pyrroline-(1-^{15}N)-1-oxyl **1b**, which presumably formed *via* the exchange of deuterium to protium during bromination in acetic acid and the Favorskii rearrangement, one can estimate the concentration of **1a** and **1b** at 73 and 27%, respectively.

‡ For parameters of EPR spectra of **1**, **2**, illustration of mass spectra of **1a**,**b**, L-band *in vivo* EPR spectra of **1**, **2**, see Online Supplementary Materials.

§ EPR spectra and reduction kinetics of **1** and **2** by the ascorbate anion were measured in a 50 mM phosphate buffer (pH 7.4) using a standard EPR capillary cell for water solutions. An ELEXSYS E-540 EPR spectrometer-tomograph (Bruker) equipped with an X-band microwave bridge (MW frequency was 9.88 GHz) and a high Q-factor resonator ER 4123SHQE (Bruker). Experimental conditions were the following: MW power of 20 mW, modulation frequency of 100 kHz and modulation amplitude of 0.005 mT. Temperature was 298 K for all measurements. Hyperfine coupling constants and line width were calculated using simulations of the experimental EPR spectra with the Winsim 2002 program[14] (the accuracy in calculating *a* is ±0.0001 mT). Initial concentration of nitroxides (C_0) was 0.2 mM, T = 298 K. To describe the experimental kinetic curves [Figure 2(*b*),(*c*)], corresponding time dependences of double integrals of the EPR signals were extrapolated to t = 0 s and normalized to C_0. 60 points were measured per one kinetic curve with a 30 s time interval between points. Time dependences of NR concentrations were approximated by a bimolecular second order kinetic scheme. Correlation coefficients were 0.9999±0.0004 in all cases. Reduction kinetics of **1**, **2** by mouse blood and plasma reductants was investigated using the same experimental conditions, C_0 = 0.25 mM for both spin probes. Mouse blood was selected into an Eppendorf tube containing sodium citrate (9:1) to prevent coagulation. Both biological reactants were used for experiments within 30 min after preparation.

¶ L-band EPR spectroscopy and tomography were perfomed with an ELEXSYS E-540 EPR spectrometer-tomograph (Bruker) equipped with an L-band microwave bridge (MW frequency was 1.0249 GHz), 3D gradient coils and an L-band E 540R36 resonator (FOV 20×20 mm). The parameters of 2D EPR images were the following: field of view, 20×20 mm; gradient strength, 0.4047 mT cm^{-1}; MW power, 113.8 mW; modulation frequency, 100 kHz; modulation amplitude, 0.05 mT; number of projections, 38. To obtain 2D EPR images, the protocols of deconvolution and back projection were used, which are a part of the Bruker Xepr 2.6b.50 software.

†† Sexually mature male mice from the SPF-vivarium of SB RAS weighing 20–25 g were used in the EPRI experiments. Mice were anesthetized by intraperitoneal injection with sodium thiopental (dose 0.6 mg kg^{-1}). All research involving laboratory animals was carried out in accordance with The Guidelines for the Care and Use of Laboratory Animals. Mice were housed in appropriate caging facilities and allowed food and water *ad libitum*.

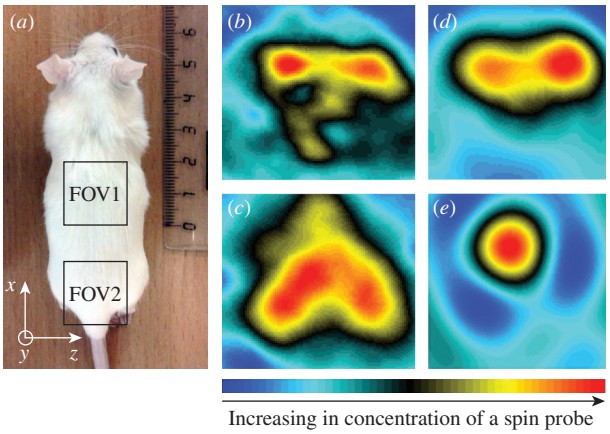

Figure 3 (*a*) Fields of view (FOV) and corresponding L-band EPR images with a spin probe of **1** (FOV1): (*b*) *zy* projection, (*c*) *zx* projection; (*d*) with a spin probe **2** (*zy* projection) and (*e*) EPR image with FOV2, illustrating the accumulation of **1** in mouse bladder 90 min after the tail vein injection of **1**.

of **1** and **2** in the middle part of a mouse body decreases mainly due to the transfer of spin probes by bloodstream. The subsequent pharmacokinetics of **1**, **2** consists in the removal of spin probes from the body by kidneys with final accumulation in bladder [Figure 3(*e*)], which is a usual phenomenon in EPR imaging.[15]

Thus, both 3-carboxy-2,2,5,5-tetra($^2H_3$)methyl-[4-^{2}H(^{1}H)]-3-pyrroline-(1-^{15}N)-1-oxyl **1** and its non-deuterated ^{14}N-containing analogue **2** demonstrate relatively high retention times in mice, allowing for EPRI experiments for more than 1 h. The use of spin probe **1** afforded better resolved images, compared to those obtained with **2**. Both nitroxides may be considered as basic structures for the molecular design of specifically targeted molecular probes for EPRI.

This work was supported by the Russian Foundation for Basic Research (project no. 12-03-00718-a) and the Ministry of Education and Science of the Russian Federation within a Project of Joint Laboratories of the Siberian Branch of the Russian Academy of Sciences and National Research Universities. We are grateful to Professor T. G. Tolstikova and Dr. M. V. Khvostov (N. N. Vorozhtsov Novosibirsk Institute of Organic Chemistry, SB RAS) for their invaluable help on working with animals.

Online Supplementary Materials

Supplementary data associated with this article can be found in the online version at doi:10.1016/j.mencom.2014.09.017.

References

1 H. J. Halpern, D. P. Spencer, J. van Polen, M. K. Bowman, R. J. Massoth, A. C. Nelson, E. M. Dowey and B. A. Teicher, *Rev. Sci. Instrum.*, 1989, **60**, 1040.
2 V. V. Khramtsov, in *Nitroxides – Theory, Experiment and Applications*, ed. A. I. Kokorin, InTech, 2012, ch. 11, p. 317.
3 G. I. Likhtenshtein, in *Nitroxides: Applications in Chemistry, Biomedicine and Material Science*, eds. G. I. Likhtenshtein, J. Yamauchi, S. Nakatsuji, A. Smirnov and R. Tamura, Wiley-VCH, Weinheim, 2008, ch. 11, pp. 371–400.
4 S. R. Burks, J. Bakhshai, M. A. Makowsky, S. Muralidharan, P. Tsai, G. M. Rosen and J. P. Y. Kao, *J. Org. Chem.*, 2010, **75**, 6463.
5 H. M. Swartz, *Free Radical Res. Commun.*, 1990, **9**, 399.
6 I. A. Kirilyuk, Yu. F. Polienko, O. A. Krumkacheva, R. K. Strizhakov, Yu. V. Gatilov, I. A. Grigor'ev and E. G. Bagryanskaya, *J. Org. Chem.*, 2012, **77**, 8016.
7 V. V. Khramtsov and L. B. Volodarsky, in *Biological Magnetic Resonance*, ed. L. J. Berliner, Plenum Press, New York, 1998, vol. 14, pp. 109–178.
8 H. J. Halpern, Yu. Cheng, M. Peric, E. Barth, D. Grdina and B. A. Teicher, *Proc. Natl. Acad. Sci. USA*, 1994, **91**, 13047.
9 J. F. W. Keana and F. L. Van Nice, *Physiol. Chem. Phys. Med. NMR*, 1984, **16**, 477.
10 Y. Lin, W. Liu, H. Ohno and T. Ogata, *Anal. Sci.*, 1999, **15**, 973.
11 A. A. Bobko, I. A. Kirilyuk, I. A. Grigor'ev, J. L. Zweier and V. V. Khramtsov, *Free Radical Biol. Med.*, 2007, **42**, 404.
12 J. Pirrwitz and D. Schwarz, *DDR Patent*, 222017 A1 (WP C 07 D/260 901 6).
13 E. G. Rozantsev, *Free Nitroxyl Radicals*, ed. H. Ulrich, Plenum Press, New York, 1970.
14 D. R. Duling, *J. Magn. Reson.*, 1994, **104**, 105.
15 C. R. Haney, A. D. Parasca, K. Ichikawa, B. B. Williams, M. Elas, C. A. Pelizzari and H. J. Halpern, *Mol. Imaging*, 2006, **5** (3), 175.

Received: 20th January 2014; Com. 14/4288